Column-in-valve designs to minimize extra-column volumes

Pepermans, Vincent; Rerick, Michael T.; Degreef, Bart; Eeltink, Sebastiaan; Weber, Stephen G.; Desmet, Gert

Published in:
Journal of Chromatography A

DOI:
10.1016/j.chroma.2020.461779

Publication date:
2021

Column-in-Valve Designs to Minimize Extra-Column Volumes

Vincent Pepermans[1], Michael T. Rerick[2], Bart Degreef[1], Sebastiaan Eeltink[1], Stephen G. Weber[2], Gert Desmet[1,*]

[1]*Department of Chemical Engineering, Vrije Universiteit Brussel, Brussels, Belgium*

[2]*Department of Chemistry, University of Pittsburgh, Pennsylvania, USA*

[(*)] Corresponding author E-mail: gedesmet@vub.be

Keywords: extra-column dispersion, column fabrication, rotor-stator valve, column hardware

Abstract

We report on the design and performance of in-house built column cartridges that can be directly screwed into the ports of a commercial rotor-stator valve to minimize extra-column band broadening and pressure-drop losses when pursuing ultra-fast separations such as those needed in 2D and 3D-LC separations. Two basic designs were evaluated and were compared with the results obtained with a commercial screw-in column cartridge. The system produces an extra-column band broadening as low as 0.05 to 0.1 μL^2 for the employed UV-detector set-up. Despite these very low values, the obtained separation efficiency of the in-house fabricated cartridge columns was very low, corresponding to a reduced minimal plate height around h=7 at the very best, which, for the 1.7 μm particle and 26.4 mm long columns corresponds to a number of theoretical plates of N=2200 under isocratic conditions. A similar poor performance was obtained with a commercial column cartridge with similar dimensions using the same set-up. One possible explanation of the observed performance could be found in the inner diameter of the column cartridges (i.d. =0.75 mm and 1 mm) which, for the employed sub 2-μm particles, falls into a region of column diameters that, according to literature models, is most likely to suffer from inherent packing problems.

1. Introduction

In chromatography, high speed separations require small particles packed in short columns that are eluted at high speeds [1-5]. The most advanced solutions currently used in practice typically consist of sub-2 µm (core-shell) particles (sizes down to 1.3 µm are commercially available) packed in 2.1x50 mm columns. Peaks eluting from such columns are so narrow their resolution is inevitably degraded by the extra-column band broadening experienced in the injector, in the tubing before and after the column, in the column end-fitting pieces and in the detector [6-8]. Since extra-column pressure drop increase inversely proportionally with the 4th power of the diameter of the connection tubing at constant flow rate, the possibilities to reduce the diameter of the connection tubing are limited [9]. Consequently, the most profound approach to alleviate the extra-column band broadening is to shorten the length of this tubing, or, even better, to completely eliminate it. Extra column band broadening is also a critical issue when transferring fractions from the 1D to the 2D column in 2D-LC. Even in the recently proposed, very compact set-up developed by the Armstrong group to perform sub-second separations [10], still some part of connection between valve and column is present.

In the present contribution, we therefore discuss the possibility to develop column hardware that can be directly screwed into the ports of the commercial rotor-stator valves that are currently being used as injector or as the modulator in 2D separations, hence virtually eliminating all precolumn dead times and extra-column dispersion sources (Fig. 1). The concept is similar to an approach already proposed on paper in 1983 by Erni [11]. However, to the best of our knowledge, no experimental results have been reported for the system they proposed.

We report on a feasibility study of the column-in-valve concept using current state-of-the-art particle sizes and rotor-stator valves. For this purpose, we used CNC (Computer Numerical Control) milling and drilling to produce several prototypes of column hardware with external screwing thread fitting directly into the ports of a high-speed rotor-stator injector valve. The columns were home-packed with high quality sub-2 µm particles. Column lengths were kept very short (order of 2-3 cm), to prepare for a new era of enhanced separation speeds, such as these needed in sensor-like applications [10] or as the 3rd dimension in 3D separations. The results obtained with the two different designs of the home-built screw-in column were compared with those obtained with a commercial cartridge column functioning according to the same screw-in principle. Experiments were conducted in two labs, one at the University of Pittsburgh (UoP) and one at the Vrije Universiteit Brussel (VUB) in Belgium, using two similar set-ups, differing only in the injection mode (255 nL loop injection versus 100 nL in-valve groove injection) and the detector mode (electrochemical detection versus UV-Vis detection).

2. Materials and methods

2.1 Column fabrication

Column cartridges were fabricated starting from full stainless steel cylinders into which circular holes (i.d. 0.75 mm) were drilled using a CNC drill mill. For prototype 2, both sides of the column cartridges have 1/16” thread and are capped with 1/16” ferrules (Valco Instruments Co., Houston, Texas). Prototype 1 had only a 1/16” ferrule at the inlet and was connected straight to the detector capillary with a IsoBar

Systems frit assembly (IDEX Health and Science, Oak Harbor, Washington), whereas Prototype 2 was connected via a 150 µm bore, 1/16" union (Valco Instruments Co., Houston, Texas) with a 1/16", 0.5 µm pore size, 0.75 mm thickness stainless steel frit (Valco Instruments Co., Houston, Texas). These frits were later replaced by a 0.075 mm thickness stainless steel screen (Valco Instruments Co., Houston, Texas).

The column at the UoP was packed with a Haskel model DSF-150 pneumatic amplification pump (Burbank, California) connected to a stainless steel slip-type union (Model 60-21HF4-U, High Pressure Equipment, Erie, Pennsylvania) that held the stationary phase slurry (80 µL). The stationary phase-containing union was connected to the inlet of the cartridge column. At the end of the column, a 150 µm ID, 360 µm OD fused silica capillary (Polymicro Technologies, Phoenix, Arizona) was used as restrictor. The columns were packed by pressurizing to 18.000 psi, holding it for 15 minutes and then cutting the airflow to the Haskel pump so the pressure slowly decreased to zero. This process was repeated 2 times. To prepare the slurry solvent, isopropanol (Certified ACS Plus isopropyl alcohol – Fisher Scientific, Fair Lawn, New Jersey) was mixed with the stationary phase (Acquity BEH C18, 1.7 µm particles, Waters Corp., Milford, Massachusetts) to get a 200 mg/ml suspension. Methanol (Biosolve, Valkenswaard, The Netherlands) was used for the packing solvent.

For the packing at the Vrije Universiteit Brussel (VUB), the same conditions were used with the exception that a high pressure resistant slurry container (60-21HF4, HiP, Erie, Pennsylvania) was used with a 100 µm ID, 360 µm OD fused silica capillary restrictor. To improve the packing process, a vibrating shaker was connected to the column, using continuous vibrations to stack the particles as efficiently as possible.

To compare with a commercial cartridge system, EXP LC Guard columns (L=5 mm, i.d.=1 mm, d_p=1.8 µm, Optimize Technologies, Oregon City, Oregon) were used.

2.2 Chromatographic set-up and methods

At the University of Pittsburgh the instrument consisted of a LC-30AD parallel double-plunger pump (Shimadzu, Canby, Oregon), a 2-position, 6-port UHPLC valve (C82X-6674EH, Valco, Houston, Texas) with a 255 nL injection loop (130x0.05 mm fused silica capillary, Polymicro Technologies, Phoenix, Arizona). For sample injection an infuse/withdraw PHD 4400 Hpsi programmable syringe pump (Harvard Instruments, Holliston, Massachusetts) was used with a 1 mL gastight syringe (Model 1001 TLL PTFE Luer Lock, Hamilton, Reno, Nevada). For detection, an electrochemical detector with a radial flow cell (MF-1091) was used (BASi, West Lafayette, Indiana).

In the Brussels set-up, the cartridge column was connected to an Agilent chromatographic system (Santa Clara, United States) consisting of a binary pump (Agilent 1290 Infinity Bin. Pump, G4220A), a DAD-detector (Agilent 1260 Infinity DAD VL+, G1315C) with an 80 nL flow cell, and an autosampler (Agilent 1290 Infinity Sampler, G4226A). The autosampler was bypassed by a 2-position 4-port valve (C84U-1674-.1D, Valco, Houston, USA) with an internal sample volume of 100 nL for injections. For minimal dispersion, the end of the column was connected to the detector by a 12 cm capillary (50 µm i.d., Polymicro Technologies, Phoenix, Arizona).

Acetonitrile (ACN, HPLC supra-gradient quality) was purchased from Biosolve B.V. (Valkenswaard, The Netherlands). Deionized HPLC-grade water (≤ 0.055 µS @ 25°C) was produced using a Milli-Q water

purification system equipped with a 0.22 µm filter (Millipore, Molsheim, France). To test the performance of the column, a 100 ppm sample containing ethylparaben and propylparaben in the isocratic solvent composition was prepared from a 1000 ppm stock sample.

The sample was injected onto the column using flow rates ranging from 5-100 µL/min, 70:30% (v/v) H_2O:ACN (VUB) and 80:20% (w/w) H_2O:ACN (UoP), to form van Deemter curves. After injection, the valve was switched in-line and the sample flowed to the column with almost no dead volume in between (except the bore volume). From the column, the sample goes through the capillary (VUB: L=12 cm, i.d.=50 µm, UoP: L=4 cm, i.d.=50 µm) to the detector.

3. Results and discussion

3.1 Column design and fabrication

The column cartridges were home-made, using a CNC drill mill to drill a cylindrical hole through a solid metal cylinder. As revealed by SEM (Scanning Electron Micrograph) analysis, it proved to be very difficult to maintain a perfect concentricity of the bore along the tube length, leading to columns where the bore does not run parallel with the tube axis (see Fig. S-1 in Supporting Material SM), in turn inevitably causing some misalignment with the connection piece at either of both column ends and the formation of a dead zone at the interface with the column frit.

Two basic designs, further referred to as Prototype 1 and 2, were considered (Fig. 2). The main difference between both designs was the frit used at the column outlet. In Prototype 1, the frit fits into a commercial filter holder with 0.51 mm diameter, which is smaller than the actual diameter of the column 0.742 mm. Obviously, this is not an ideal situation given the creation of dead zones at the outer ring of the column outlet [12,13]. In Prototype 2, an opposite situation was created, using a frit with a 1.6 mm diameter in combination with a column with the same 0.742 mm inner diameter as in Prototype 1.

Since the obtained column efficiencies were suboptimal, several packing strategies were adopted and compared, leading to the procedure described in the experimental sections. Variations included changing the slurry solvent (acetone, methanol and hexane were considered next to the finally selected isopropanol), the number of process repeats (ranging between zero and two) and the pressure (ranging between 1000 and 1500 bar). Eventually, the packing process was also carried out using an external shaking device placed against the column to generate continuous vibration during the high-pressure phase of the packing. No significant improvement in packing quality was however observed.

3.2 System assembly and characteristics

The final assembled system with the column screwed into the valve was only arranged with a frit at the column outlet. Therefore, the valve was mounted upside down to prevent backflow of the particles when the flow was switched off. To minimize the volume in the connection tubing leading to the detector, the distance to the detector was minimized, reducing it to only 12 cm in the Brussels set-up and even only 4 cm in the Pittsburgh set-up.

The column-in-valve systems were intensively tested in two different labs, one at the University of Brussels and one at the University of Pittsburgh. Prior to the actual chromatographic experiments, the system was first characterized without the column in place to determine the system volume and its variance. For this purpose, 100 nL (Brussels set-up) and 255 nL (Pittsburgh set-up) sample volumes were injected into a 70:30% (v/v) H_2O:ACN (VUB) and 80:20% (w/w) H_2O:ACN (UoP) mobile phase at various flow rates in both the Brussels set-up (in-valve injection, UV-Vis detection) and the Pittsburgh set-up (sample loop injector, electrochemical detection). The results are shown in Fig. 3 for both the 80 nL UV-Vis detector and electrochemical detector. As can be noted from Fig. 3, the effect of the detector's cell volume on the extra-column peak is significant, as the set-up equipped with the electrochemical detector (Figs. 3d-e) clearly produces a longer tail than the UV-detection set-up used in Brussels (Figs. 3a-c). Determining the peaks 1^{st} order moment at different flow rates (measured t_r-values given in Table 1) and plotting these values versus the reciprocal of the flow rate (see Fig. S2 of SM with F expressed in μL/s), the slope of the obtained linear trend ($R^2 \geq 0.9997$) provides the value of the system volume. This procedure returns a value of 525 nL for the UV set-up and 811 nL for the electrochemical set-up (cf. slope values in linear trend equations shown in Fig. S2 of the SM).

The value measured for the UV-set-up is in excellent agreement with what can be expected based on the estimated dimensions of the different pieces. Using the available geometrical data, the theoretical system volume of the Brussels set-up was estimated to be 510 nL (vs. 525 nL experimentally), a value by adding the nominal 100 nL for the injection groove, 50 nL of flow circuitry inside the injector valve (volume of bore between injection groove and seating of column inlet as derived from the manufacturer's information), 240 nL for the connection tubing (i.d.=0.05 mm and L=12 cm) and 40 nL for the flow circuitry of the detector and 80 nL for the detector cell itself.

The exact volume of the electrochemical detector flow cell used in the Pittsburgh set-up is difficult to determine because of the cell's outlet flow path, but it can be roughly calculated using the thickness of the gasket as this determines the distance between the working and counter electrodes. Doing so, the detector cell volume can be estimated to be around 90 nL. To this number, the volume of the post-column tubing (80 nL) and the detector inlet (100 nL) must be added, as well as the volume of the injection loop (255 nL) and the volume of the intra-valve flow circuitry (estimated to be 50 nL as derived from the manufacturer's information). Combined, this makes up a volume of 575 nL, which is similar to the Brussels set-up, but about 30% smaller than the measured volume (810 nL). A possible explanation for this deviation could be that the reported retention times are determined via calculation is based on the method of moments, which is comprised by the long tail of the electrochemical responses which makes it difficult to correctly determine the integration boundaries. This longer tail probably originates from the fact that, in order to keep mobile phase composition comparable between systems, no salt was added to the mobile phase in the Pittsburgh set-up as is common with electrochemical studies. This would lead to a larger electrical resistance within the flow cell, resulting in a more strongly tailed signal response. Another source of tailing obviously could be the incomplete diffusion relaxation between different velocity regions in the laminar flow system

Important to remark in Fig. S2 is the relatively large value of the offset on the y-axis, indicative of the response delay time. This delay amounts up to about 500 ms for the UV-set-up and 1000 ms for the

electrochemical set-up. The 500 ms delay time measured for the UV-set-up, the delay times most probably originate from the finite valve switching electronic response times. The additional response time observed for the electrochemical detector can be fully owed to the 1.0 Hz Butterworth filter, the fastest filter inherent to the BASi potentiostat, from which a constant signal delay of about 0.6 seconds is expected.

Turning now to the system variance, Table 1 gives the 4σ-based variances of the system peaks shown in Fig. 3, it can be noted these are typically in the order of some 0.05 to 0.09 μL^2 for the Brussels set-up and some 0.09 to 0.26 μL^2 for the Pittsburgh set-up, with the larger values for the highest flow rate, which can be expected because the system can be considered as open-tubular system which, given the applied flow rates, is operated in the flow dispersion dominated regime. The observed volumetric system variances are clearly smaller than the system variances typically reported for the best commercial low-dispersion UHPLC systems (typically 1-20 μL^2 [7,14-19], owing to the use of small injection volumes (100 nL in-valve injection groove arranged in a rotor-stator valve with internal bores of 100 μm, the smallest bore commercially available), short (12 cm) and narrow (50 mm i.d.) connection tubing and the use of a 80 nL-detector UV-Vis detector.

The 4σ-based system variances in the Pittsburgh set-up are larger, mostly owing to the strong tail of the system peaks (cf. Figs. 3d-e) as can be assessed from the peak asymmetry factors measured at 10% height. These vary between AF=8.3 at 20 μL/min AF=4.4 at 100 μL/min. The tailing can also be assessed from the large difference between the 4σ-based variances and those obtained at the peak half heights (see last column in Table 1).

3.3 Pressure drop and flow stability

It was our initial experience that the use of both Prototype 1 and 2 columns led to a fast increase in pressure (10-20 bars per hour), a problem which was often accompanied by a strong decrease in plate number. This flow instability was presumably due to clogging of the frits, as was supported by a SEM-analysis of the frits (Fig. S-1d). To resolve this, all later generation devices used a 0.075 mm thick stainless-steel screen frit. This solved the pressure increase/clogging and partly solved the decrease in column efficiency over time.

The maximal flow rate applied to the column cartridges was 200 μL/min, corresponding to an inlet pressure of about 1000 bar, without any leakage problems. However, further increasing the flow rate to 240 μL/min typically made the system fail by disconnecting the loop capillary from its sleeve and ferrule, while the column was still connected to the valve. Fig. 4 shows the relation between the measured total pressure drop and the flow rate. Except for the highest flow rate (where the corresponding Reynolds number is on the order of 650, hence approaching the onset of turbulence), the data points follow a linear relationship, in agreement with the theoretical expectations. Calculating the column permeability from the slope of the linear relationship using Darcy's law:

$$K_{V0} = u_0 \cdot \eta \cdot \frac{L}{\Delta P} \quad (1)$$

wherein u_0 is the mobile phase velocity, η the mobile phase viscosity, L the column length and ΔP the pressure drop, we find a value of K_{v0}=1.5 10^{-10} m^2, corresponding to a t_0-based flow resistance of $\phi_0=d_{part}^2/K_{v0}$=1900. With the pressured-drop of the system (=no column in place) amounting only up to 0.3% of the pressure-drop measured with the column in place, the extra-column pressure drop can be clearly neglected. The ϕ_0= 1900 is more than a factor of 2 higher than expected for a packed bed of spheres, indicating a poor column packing quality.

3.4 Chromatographic performance

Fig. 5 shows representative chromatograms obtained with the three tested systems. As can be noted, retained peaks have an acceptable symmetry (AF=1.22 for peak 2 and AF=1.15 for peak 3, using the 10% height definition for AF). The unretained peak around the column's t_0-time on the other hand is highly skewed.

Figs. 6 shows the reduced plate height plots ($h=H/d_p$ with d_p=1.7 μm versus $\nu=u.d_p/D_{mol}$ with D_{mol}=9.8·10^{-10} m^2/s) for peak nr. 2 (ethylparaben). Very similar data were obtained for peak nr. 3 (propylparaben). Obviously, the observed plate heights are much larger than the h≅2-values typically cited in literature for well-packed fully porous particle columns [20-22]. To investigate to which extent the high observed plate heights are influenced by the extra-column contributions in this minimal-volume system, we can compare the volumetric variances measured with the column in place (for peak nr. 2 on the order of σ_V^2=2.3 mL^2 at 20 mL/min and σ_V^2=13.6 mL^2 at 100 mL/min in the best performing column) with the system-only variances obtained in Section 3.2. From the values cited there (see also Table 1), it can be concluded that the plate height values shown in Fig. 6 are only influenced by the extra-column band broadening for 10% at most, such that it can be surmised that the explanation for the very high degree of band broadening should not be sought in the extra-column dispersion occurring in the valve, the connection tubing or the detector.

Another presumed potential additional source of band broadening, albeit with a magnitude that is difficult to assess, can be found in the fact that in none of the fabricated and tested prototypes the bore axis was running sufficiently parallel with the tube axis, inevitably creating a dead zone at the interface with the frit at the column outlet. To verify this hypothesis, we also used a commercially fabricated cartridge column (EXP LC Guard column, L=5 mm, I.D.=1 mm, d_p= 1.8) with similar dimensions. As can be noted from the grey data points added to Fig. 6b, a nearly identical performance is obtained as for Prototype 2. A specific reason for the near perfect coincidence of both curves is, given the low contribution of the system band broadening, difficult to conceive. Nevertheless, it points out that the skew of the bore axis in the in-house fabricated cartridges is not necessarily an important contributor to the observed high h-values.

To analyze the reduced van Deemter curves in more detail, looking for a further potential explanation of the high observed plate heights, the reduced plate height curves have been fitted with the well-established van Deemter-model [23]:

$$h = A + B/\nu + C \cdot \nu \qquad (2)$$

For Prototype 1 the A-, B-, C-values were determined to be A=4.81, B=10.63, C=0.78, for Prototype 2 we found A=1.14, B=10.60, C=1.04, and for the commercial cartridge column we found A=0, B=11.37, C=1.30. Because of an insufficient number of data points in the B-term range for the Prototype 2-data, the data fit for this series was carried out using the B-term value obtained for Prototype 1. The difference in A-term contribution between both prototypes is striking: while the A=1.14 for the Prototype 2-columns can be considered as acceptable for a home-packed column, the A=4.81 for the Prototype 1-columns is unusually large. The A-term is supposed to reflect differences in packing quality. Possibly, the fact that in Prototype 1 the packing solvent can only leave the column through the central zone (corresponding to the 0.51 mm diameter frit) while there is an outer ring of the column bed forming a dead-end for the packing solvent and thus creating strong radial differences in local packing density and structure, might explain this very high A-value. The larger frit used in Prototype 2-columns prevents the occurrence of such a dead end-zone during column filling, which thus might explain the lower A-term value compared to that obtained for Prototype 1-columns. The A=0-value obtained for the commercial column could be due to an insufficient B-term fit, as we have only one data point at a sufficiently low velocity.

Also striking are the large C-term constants, typically on the order of 0.05 in a state-of-the-art well-packed column [21], and here more than an order of magnitude larger. This would in the older literature on plate height modelling [20] have been attributed to an excessive mass transfer resistance, but it is now a well-established fact that radial velocity differences (induced by packing inhomogeneities) that persist over a sufficiently long distance also generate a C-term like behavior (i.e., showing a quasi-linear variation between h and ν) [24-26]. As explained by Gritti [27-28], the inevitable difference in packing density between the wall region and the central region is a tenuous cause of such radial velocity differences. In an elegant analysis in [27], starting from the fact that the thickness of this wall region can be assumed more or less constant, Gritti showed that the contribution to band broadening of this wall region would, for the presently considered case of 2 μm particles, be most pronounced in column diameters ranging between 0.30 mm and 2.0 mm. As a matter of fact, the currently employed cartridge format (0.75 mm i.d.) is, in hindsight, about one of the worst possible column i.d.'s, as it lies near the maximum in the curve of h_{min} versus column diameter given in Fig. 6 of [27-28], a maximum lying around h_{min}=4.5, instead of around the h_{min}=2 that can be reached in d_c=2.1 and 4.6 mm. This hence already explains part of the high plate heights observed in the present study. The diameter of the commercial cartridge column (1 mm i.d.) is situated near the top of this h_{min}-curve as well, thus probably explaining why similar h-values are obtained as with the Prototype 2 results.

4. Conclusions

To minimize the system volumes in ultra-fast UHPLC separations, it is possible to eliminate the tubing between column and injector by directly screwing a column cartridge with external screw-thread into the ports of a rotor-stator injector valve. In the present work, this has been implemented using in-house fabricated and packed column cartridges. Although the resulting system dispersion is very small (ranging between 0.05 and 0.1 μL^2 for the employed UV-detector set-up), the observed separation efficiencies are very low, with high h_{min}-values and steep C-term parts of the plate height curves: h_{min}=10.5 and C-term=0.78 for Prototype 1 and h_{min}=7 and C-term=0.88 for Prototype 2.

At present, we attribute a large part of the observed poor efficiency to the format of the employed cartridges, more specifically to their inner diameter, falling amidst the range of diameters identified as inherently impossible to pack well by Gritti [27,28]. Using cartridges with either a wider bore therefore seems the best way forward, as the other option, i.e., use columns with a much narrower bore, would be compromised by the fact these are more influenced by the extra-column dispersion and are tedious to pack. Other contributing factors could be found in the tilted axis of the cartridge bores, the non-matching frit dimensions and the perceived clogging of the frits.

Acknowledgements

I would like to acknowledge the Excellence of Science (EOS) program (grant nr. 30897864) funded by FWO-FNRS for making this research possible.

References

[1] A.S. Kaplitz, G.A. Kresge, B. Selover, L. Horvat, E.G. Franklin, J.M. Godinho, K.M. Grinias, S.W. Foster, J.J. Davis, J.P. Grinias, High-Throughput and Ultrafast Liquid Chromatography, Anal. Chem. 92 (2020) 67−84.
doi: 10.1021/acs.analchem.9b04713

[2] J. Destefano, T. Langlois, J. Kirkland, Characteristics of superficially-porous silica particles for fast HPLC: some performance comparisons with sub-2-µm particles, J. Chromatogr. Sci. 46 (2008) 254-260.
doi: 10.1093/chromsci/46.3.254

[3] S. Fekete, E. Oláh, J. Fekete, Fast liquid chromatography: the domination of core–shell and very fine particles, J. Chromatogr. A, 1228 (2012) 57-71.
doi: 10.1016/j.chroma.2011.09.050

[4] S. Fekete, D. Guillarme, Kinetic evaluation of new generation of column packed with 1.3 µm core-shell particles, J. Chromatogr. A. 1308 (2013) 104–113.
doi:10.1016/j.chroma.2013.08.008.

[5] C.L. Barhate, M.F. Wahab, Z.S. Breitbach, D.S. Bell, D.W. Armstrong, High efficiency, narrow particle size distribution, sub-2 µm based macrocyclic glycopeptide chiral stationary phases in HPLC and SFC, Analytica Chimica Acta 898 (2015) 128-137.
https://doi.org/10.1016/j.aca.2015.09.048

[6] K.J. Fountain, U.D. Neue, E.S. Grumbach, D.M. Diehl, Effects of extra-column band spreading, liquid chromatography system operating pressure, and column temperature on the performance of sub-2µm porous particles, J. Chromatogr. A 1216 (2009) 5979-5988.
doi:10.1016/j.chroma.2009.06.044

[7] S. Fekete, J. Fekete, The impact of extra-column band broadening on the chromatographic efficiency of 5cm long narrow-bore very efficient columns, J. Chromatogr. A 1218 (2011) 5286-5291.
doi:10.1016/j.chroma.2011.06.045

[8] A. Goyon, D. Guillarme, S. Fekete, The importance of system band broadening in modern size exclusion chromatography, J. Pharm. Biomed. Anal., 135 (2017) 50-60.
http://dx.doi.org/10.1016/j.jpba.2016.12.004

[9] G. Desmet, K. Broeckhoven, Extra-column band broadening effects in contemporary liquid chromatography: Causes and solutions, TrAC Trends in Anal. Chem. 119 (2019) 115619.
https://doi.org/10.1016/j.trac.2019.115619
[10] D.C. Patel, M.F. Wahab, T.C. O'Haver, D.W. Armstrong, Separations at the Speed of Sensors, Anal. Chem. 90 (5) (2018) 3349-3356.
[11] F. Erni, The limits of speed in high-performance liquid chromatography, J. Chromatogr. A 282 (1983) 371-383.
https://doi.org/10.1016/S0021-9673(00)91615-7
doi: 10.1021/acs.analchem.7b04944
[12] K. Broeckhoven, K. Vanderlinden, D. Guillarme, G. Desmet, On-tubing fluorescence measurements of the band broadening of contemporary injectors in ultra-high performance liquid chromatography, J. Chromatogr. A 1535 (2018) 44-54.
doi: 10.1016/j.chroma.2017.12.032
[13] S. Deridder, G. Desmet, K. Broeckhoven, Numerical investigation of band spreading generated by flow-through needle and fixed loop sample injectors, J. Chromatogr. A 1552 (2018) 29-42.
doi: 10.1016/j.chroma.2018.04.001
[14] F. Gritti, G. Guiochon, On the extra-column band-broadening contributions of modern, very high pressure liquid chromatographs using 2.1 mm i.d. columns packed with sub-2 μm particles, J. Chromatogr. A 1217 (2010) 7677-7689.
doi: 10.1016/j.chroma.2010.10.016
[15] F. Gritti, G. Guiochon, On the minimization of the band-broadening contributions of a modern, very high pressure liquid chromatograph, J. Chromatogr. A 1218 (2011) 4632-4648.
doi: 10.1016/j.chroma.2011.05.024
[16] T.H. Walter, R.W. Andrews, Recent innovations in UHPLC columns and instrumentation, TrAC Trends in Anal. Chem. 63 (2014) 14-20.
https://doi.org/10.1016/j.trac.2014.07.016
[17] K. Broeckhoven, G. Desmet, The future of UHPLC: Towards higher pressure and/or smaller particles?, TrAC Trends in Anal. Chem. 63 (2014) 65-75.
https://doi.org/10.1016/j.trac.2014.06.022
[18] F. Gritti, G. Guiochon, Accurate measurements of the true column efficiency and of the instrument band broadening contributions in the presence of a chromatographic column, J. Chromatogr. A 1327 (2014) 49-56.
doi: 10.1016/j.chroma.2013.12.003
[19] M. Dittmann, The issue of external band broadening in HPLC/UHPLC devices, in S. Kromidas, The HPLC expert II: Find and optimize the benefits of your HPLC/UHPLC, Wiley VCH, Weinheim, 2017.
[20] J.H. Knox, Band dispersion in chromatography – a new view of A -term dispersion, J. Chromatogr. A. 831 (1999) 3–15.
https://doi.org/10.1016/S0021-9673(98)00497-X
[21] D. Cabooter, A. Fanigliulo, G. Bellazzi, B. Allieri, A. Rottigni, G. Desmet, Relationship between the particle size distribution of commercial fully porous and superficially porous high-performance liquid chromatography column packings and their chromatographic performance, J. Chromatogr. A 1217(45) (2010) 7074-7081.

391 doi: 10.1016/j.chroma.2010.09.008
392 [22] M. Catani, O.H. Ismail, A. Cavazzini, A. Ciogli, C. Villani, L. Pasti, C. Bergantin, D. Cabooter, G. Desmet,
393 F. Gasparrini, D.S. Bell, Rationale behind the optimum efficiency of columns packed with new 1.9 µm fully
394 porous particles of narrow particle size distribution, J. Chromatogr. A. 1454 (2016) 78–85.
395 doi:10.1016/j.chroma.2016.05.037.
396 [23] U.D. Neue, HPLC columns: theory, technology and practice, Wiley-VCH, New York, 1997.
397 [24] G. Desmet, A finite parallel zone model to interpret and extend Giddings' coupling theory for the
398 eddy-dispersion in porous chromatographic media, J. Chromatogr. A. 1314 (2013) 124–137.
399 doi:10.1016/j.chroma.2013.09.016.
400 [25] F. Gritti, On the relationship between radial structure heterogeneities and efficiency of
401 chromatographic columns, J. Chromatogr. A. 1533 (2018) 112–126.
402 doi: 10.1016/j.chroma.2017.12.030
403 [26] G. Desmet, B. Huygens, W. Smits, S. Deridder, The checkerboard model for the eddy-dispersion in
404 laminar flows through porous media. Part I: Theory and velocity field properties, J. Chromatogr. A. 1624
405 (2020) 461195.
406 doi: 10.1016/j.chroma.2020.461195
407 [27] F. Gritti, A stochastic view on column efficiency, J. Chromatogr. A. 1540 (2018) 55–67.
408 doi:10.1016/j.chroma.2018.02.005.
409 [28] F. Gritti and M. F. Wahab, Understanding the Science Behind Packing High-Efficiency Columns and
410 Capillaries: Facts, Fundamentals, Challenges, and Future Directions, LC GC N-A 36(2) (2018) 82-98.
411
412

Figure captions

Figure 1. Schematic representation of the aim of the present study: replacing the conventional tubing-based connection between rotor-stator valve **(a)** by an approach where the column is directly screwed into one of the ports of a commercial rotor-stator valve **(b)**.

Figure 2. Basic column cartridge designs developed in the present study: **(a)** external view of Prototype 1; **(b)** longitudinal section cut of Prototype 1; **(c)** external view of Prototype 2; **(d)** longitudinal section cut of Prototype 2.

Figure 3. Chromatograms of the system peaks (i.e., without column in place) for the Brussels set-up **(a)** 20 µL/min, **(b)** 50 µL/min, **(c)** 100 µL/min and for the Pittsburgh set-up **(d)** 20 µL/min, **(e)** 50 µL/min, **(f)** 100 µL/min.

Figure 4. Plot of pressure drop over the as a function of the flow rate for Prototype 2 (mobile phase=80:20% (w/w) H_20:ACN).

Figure 5. (a) Example chromatograms obtained with Prototype 1, **(b)** Example chromatograms obtained with Prototype 2, **(c)** Example chromatograms obtained with commercial cartridge column.

Figure 6. Reduced plate height plots obtained with **(a)** Prototype 1 and with **(b)** Prototype 2 for Ethylparaben (mobile phase=80:20% (w/w) H_20:ACN). The grey triangles in (b) represent the corresponding data measured in the commercial cartridge column.

Table 1. *System peak characteristics*

	UV-detector set-up			Electrochemical detector set-up			
F(µL/min)	t_r(s)	σ_t^2(s^2)	σ_V^2(µL^2)	t_r(s)	σ_t^2(s^2)	σ_V^2(µL^2)	σ_V^2(µL^2) at HH
20	2.081	0.423	0.047	3.457	0.841	0.093	0.0665
50	1.149	0.109	0.075	2.010	0.208	0.145	0.1024
100	0.813	0.032	0.090	1.496	0.094	0.262	0.1662

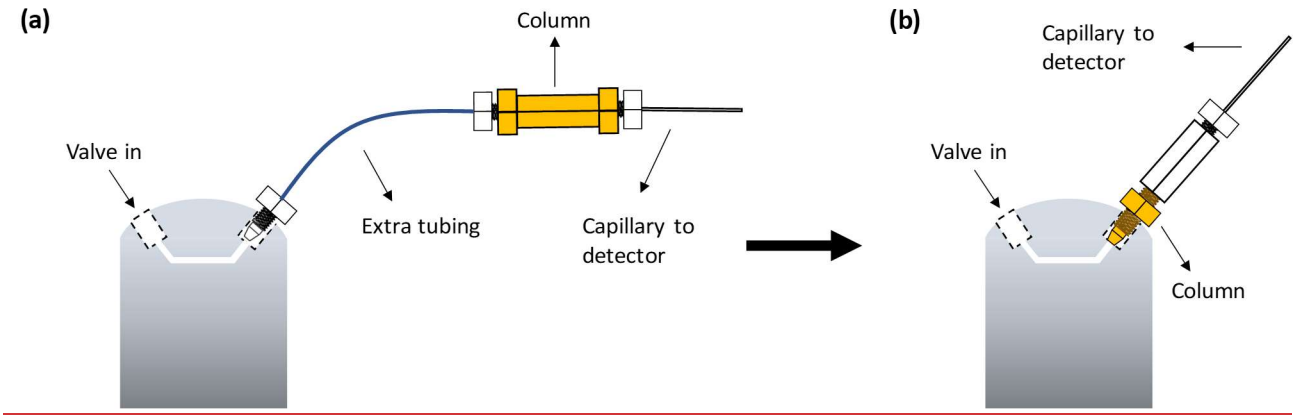
(a)
Column
Valve in
Extra tubing
Capillary to
detector
(b)
Capillary to
detector
Valve in
Column

Fig.1

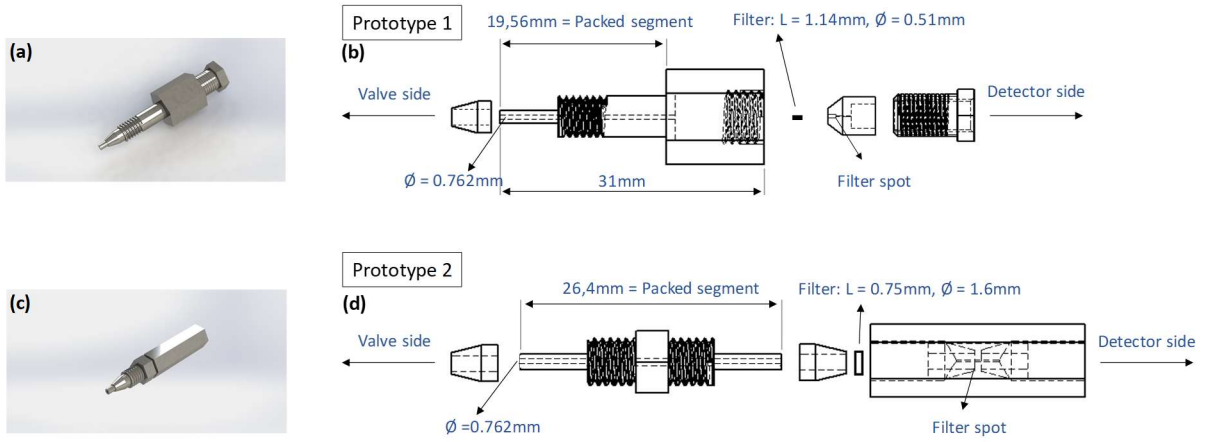
(a)
Prototype 1
19,56mm = Packed segment
Filter: L = 1.14mm, Ø = 0.51mm
(b)
Valve side
Detector side
Ø = 0.762mm
31mm
Filter spot
(c)
Prototype 2
26,4mm = Packed segment
Filter: L = 0.75mm, Ø = 1.6mm
(d)
Valve side
Detector side
Ø =0.762mm
Filter spot

Fig.2

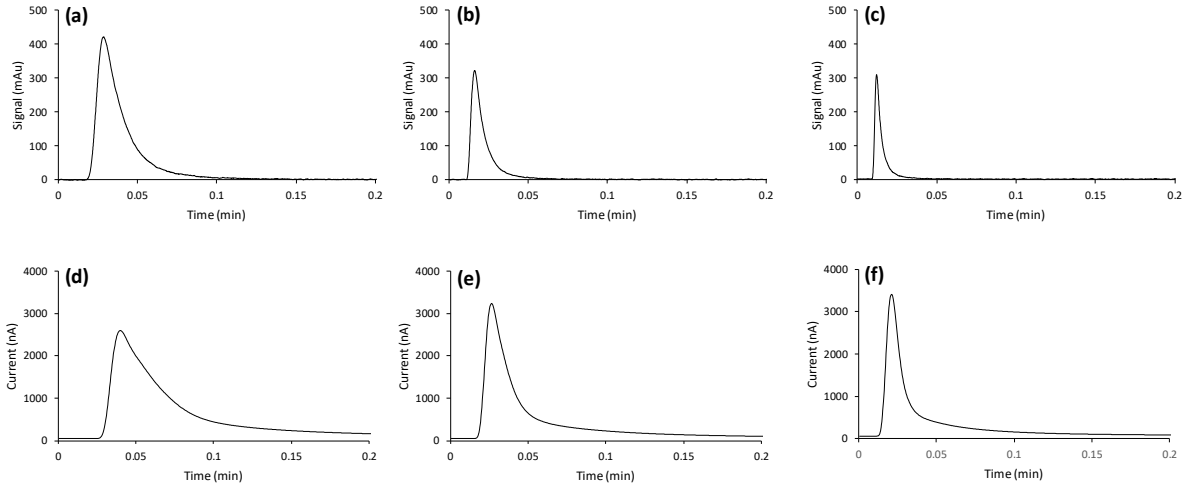

Fig.3

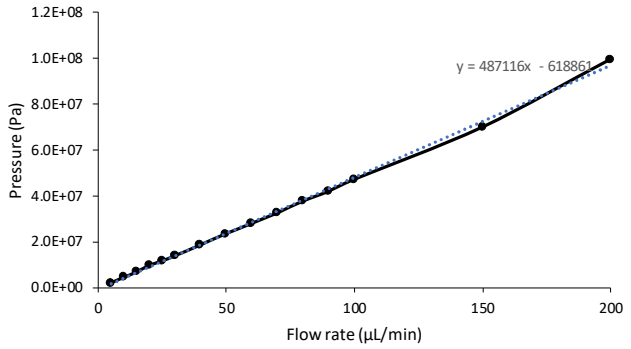
1.2E+08
1.0E+08
8.0E+07
6.0E+07
4.0E+07
2.0E+07
0.0E+00
Pressure (Pa)
y = 487116x - 618861
0
50
100
150
200
Flow rate (µL/min)

Fig.4

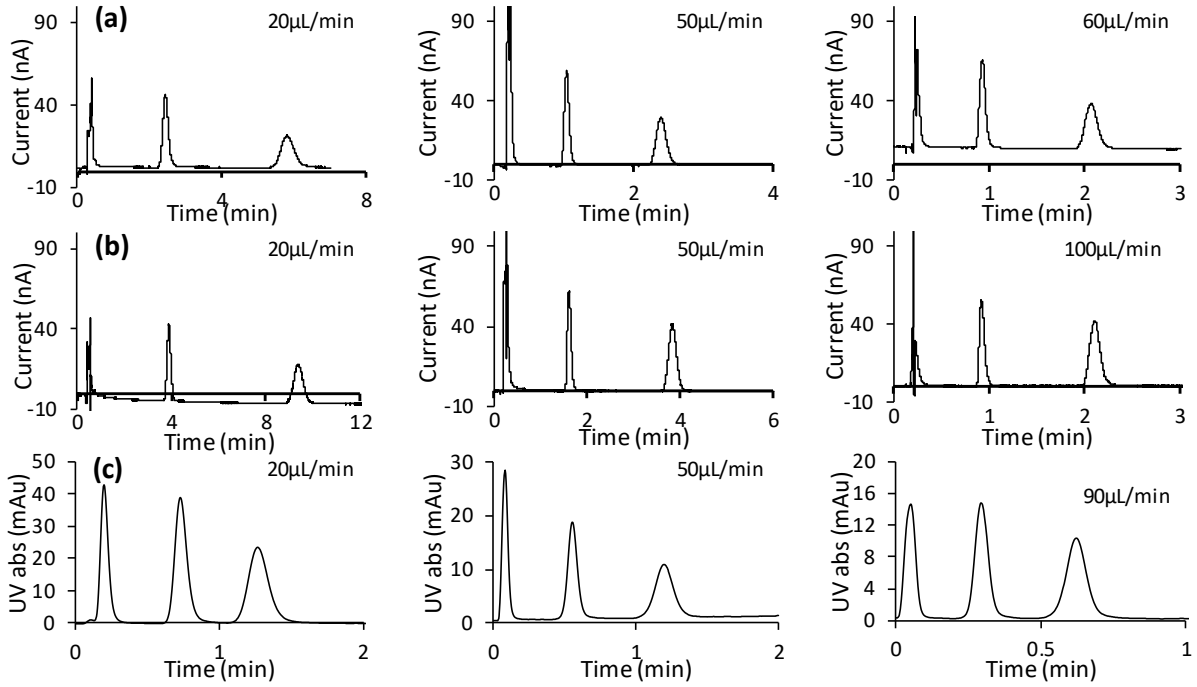
(a)
20μL/min
50μL/min
60μL/min
(b)
20μL/min
50μL/min
100μL/min
(c)
20μL/min
50μL/min
90μL/min
Current (nA)
UV abs (mAu)
Time (min)

Fig.5

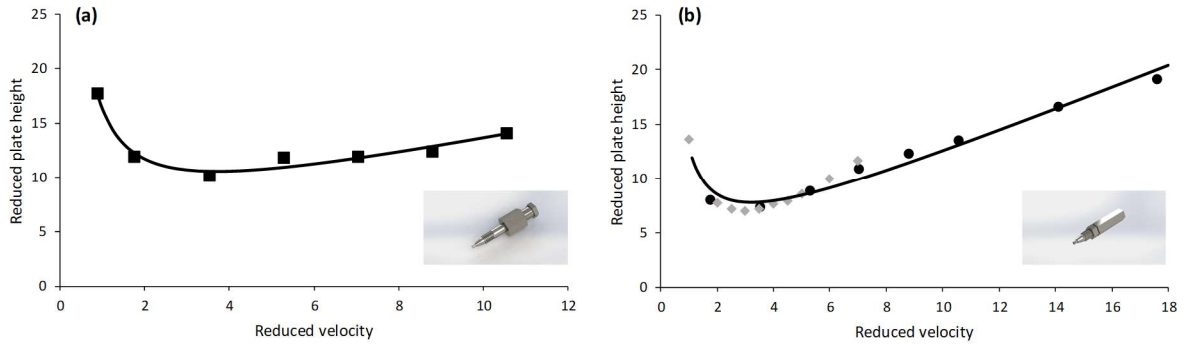
(a)
Reduced plate height
Reduced velocity
0
5
10
15
20
25
0
2
4
6
8
10
12
(b)
Reduced plate height
Reduced velocity
0
5
10
15
20
25
0
2
4
6
8
10
12
14
16
18

518

519

Fig.6